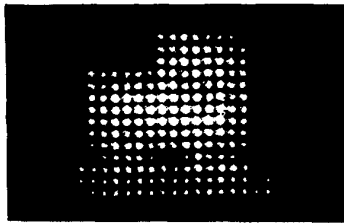


(a)



(b)

CWF60 Fig. 2 (a) An input pattern and (b) the weighted output pattern.

One of the most important applications of cellular automata is for image processing. In terms of Boolean decomposition,<sup>5</sup> the image processing functions in mathematical morphology can be directly implemented by such a cellular automaton module.

This work was supported by the NNSFC, the CAS, and the HIB.

1. J. Taboury, J. M. Wang, P. Chavel, F. Devos, P. Garda, *Appl. Opt.* **27**, 1643 (1988).
2. K. S. Huang, A. A. Sawchuk, B. K. Jenkins, P. Chavel, J. M. Wang, A. G. Weber, C. H. Wang, I. Glaser, *Appl. Opt.* **32**, 166 (1993).
3. F. A. P. Tooley, S. Wakelin, M. R. Taghizadeh, *Appl. Opt.* **33**, 1398 (1994).
4. F. A. Gerritsen, P. W. Werbeek, *Compt. Vision Graph. Image Proc.* **27**, 115 (1984).
5. L. Liu, *Opt. Eng.* **33**, 3447 (1994).

CWF61

All-optical integrated Mach-Zehnder switching in lithium niobate waveguides due to cascaded nonlinearities

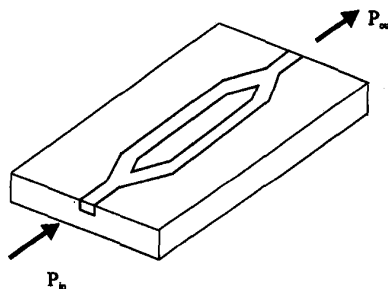
Y. Baek, R. Schiek, G. Krijnen, G. I. Stegeman, I. Baumann,\* W. Sohler,\* *Center for Research and Education in Optics and Lasers, University of Central Florida, 12424 Research Parkway, Orlando, Florida 32826*

In all-optical switching the required phase shift is produced by the light itself. Typically this phase shift has been achieved via the intensity-dependent re-

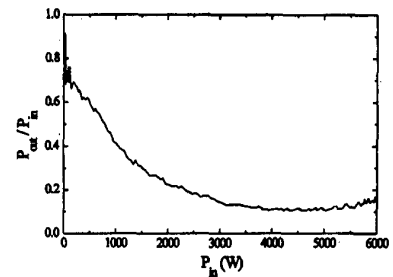
fractive index, i.e., third-order nonlinearities. But recently the fact that the so-called cascaded second-order nonlinearity can imitate the third-order nonlinearity was proved experimentally.<sup>1</sup> A phase shift in the cascaded nonlinearity is obtained through the energy exchange between a fundamental light beam and its second harmonic. In the Mach-Zehnder interferometer we need a  $\pi$ -induced phase shift for switching, which is half of the required phase shift compared to directional coupler. Previously we demonstrated switching action using a LiNbO<sub>3</sub> channel waveguide in one of the interferometer, and air in the other.<sup>2</sup> Here we report high-contrast switching in a fully integrated asymmetric Mach-Zehnder interferometer.

The experiments were performed in 49-mm-long, titanium indiffused, lithium niobate channel waveguides with propagation along the X-axis on a Y-cut crystal. An integrated Mach-Zehnder interferometer consists of two symmetric Y-junctions (Fig. 1). At the first Y-junction, the input beam is equally split into each of the two arms. In one arm, the width of the channel waveguide is tapered down from 15  $\mu\text{m}$  to 11  $\mu\text{m}$ . The separation between two arms is 80  $\mu\text{m}$ , which is wide enough to prevent linear coupling. At the second Y-junction, the light from the two channels is recombined, causing interference effects. Because of the difference in the widths of the two interferometer arms, the resonance temperature of each arm is different. This induces a different nonlinear phase shift in each arm at a fixed temperature. With small variations of the geometry we obtained an initial linear phase difference between the channels of approximately zero and  $\pi$ .

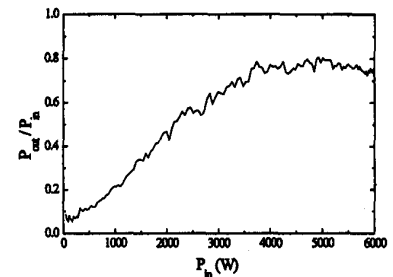
In the experiment, we used a Nd:YAG Q-switched, mode-locked laser operating at 1.32  $\mu\text{m}$  with 90-ps pulses, full-width at the half-maximum intensity. A single pulse was extracted using electro-optic pulse slicer. The sample was heated in an oven with a temperature stability of  $\pm 25$  mK to near the phase-matching temperature. The temperature profile in the oven and a slight waveguide inhomogeneity provide the nonuniform wavevector mismatch distribution along the propagation length.<sup>1</sup> Due to this nonuniform



CWF61 Fig. 1 Configuration of the integrated Mach-Zehnder interferometer.



(a)



(b)

CWF61 Fig. 2 Measured transmittance of LiNbO<sub>3</sub> integrated Mach-Zehnder interferometer as a function of the peak input power (a) initial phase at  $\sim 0$  (b) initial phase of  $\sim \pi$ .

wavevector mismatch, we can obtain large nonlinear phase shift in the small fundamental depletion region. The measured SHG tuning curves show resonance temperatures for each arm separated by 2.5 K. Figure 2 shows the outputs of the Mach-Zehnder interferometer at a fixed temperature which is in the low depletion region below both phase-matching temperatures. The output is normalized by the input power. Due to differences in the length of the arms, the switching curves start either "on" or "off." Because of the cascaded second-order nonlinearities, as we increase the input power, the output is changed from "on" to "off" or vice versa. Pulse break-up is responsible for the incomplete switching. But because of the nonlinear dependency of the phase shift on the input power in the cascaded nonlinearities we obtained a better switching ratio than using third order nonlinear materials.<sup>3</sup>

In conclusion, we demonstrated for the first time, to our knowledge, the integrated Mach-Zehnder interferometers switching due to the cascaded second-order nonlinearities with a switching ratio 8:1.

\**Angewandte Physik, Universitt Paderborn, Warburger Strasse 100, D-33098 Paderborn, Germany*

1. R. Schiek, M. L. Sundheimer, D. Y. Kim, Y. Baek, G. I. Stegeman, H. Seibert, W. Sohler, *Opt. Lett.* **19**, 1949 (1994).

- Y. Baek, R. Schiek, G. I. Stegeman, *Opt. Lett.* **20**, 2168 (1995).
- G. I. Stegeman, M. Sheik-Bahae, E. W. Van Stryland, G. Assanto, *Opt. Lett.* **18**, 13 (1993).

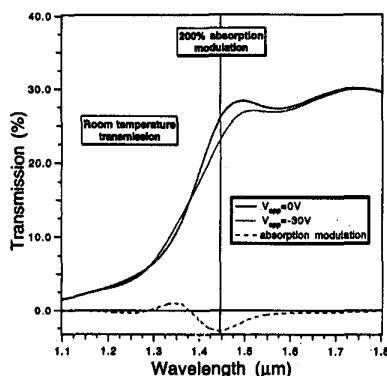
### CWF62

#### Absorption electromodulation in CdHgTe heterostructures in the 1.5- $\mu\text{m}$ range

Guido Mula, N. T. Pelekanos, P. Gentile, N. Magnea, J. L. Pautrat, *Département de Recherche Fondamentale sur la Matière Condensée, SP2M/PSC-CEA/Grenoble-17 Av. des Martyrs 38054 Grenoble Cedex 9 France*

The increasing volume of data transfer through optical telecommunication networks is demanding high-efficiency optical switches (e.g., photorefractive devices) in the wavelength range of 1.5  $\mu\text{m}$ .<sup>1</sup> Narrow-gap semiconductors like cadmium mercury telluride (CMT) are natural candidates for realizing spatial holographic interconnect of optical fibers at the telecommunication wavelengths thanks to their possibility of covering the spectral range of interest. CMT heterostructures have also the advantage of being almost lattice-matched to CdTe and  $\text{Cd}_{0.96}\text{Zn}_{0.04}\text{Te}$  substrates allowing the growth of almost strain-free devices. In the present paper we report on room-temperature transmission electromodulation in the wavelength range of 1.5  $\mu\text{m}$  of multiple quantum well (MQW) CMT heterostructures diodes.

The samples we studied consist of a 1.5- $\mu\text{m}$ -thick n-doped  $\text{Cd}_{0.96}\text{Zn}_{0.04}\text{Te}$  buffer layer, a 1.2- $\mu\text{m}$ -thick MQW active region (200- $\text{\AA}$ -thick CMT (37% Hg) wells and 100- $\text{\AA}$ -thick CMT (27% Hg) barriers), and a 100- $\text{\AA}$ -thick CdTe cap layer. The insertion of a  $\text{Cd}_{0.8}\text{Mg}_{0.2}\text{Te}$  barrier before (1000  $\text{\AA}$ ) and after (500  $\text{\AA}$ ) the active re-



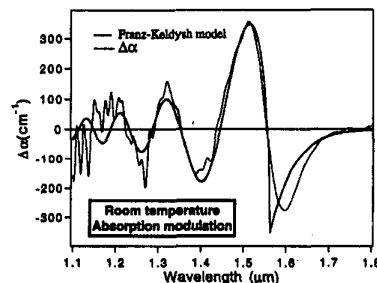
**CWF62 Fig. 1** Room-temperature transmission spectra at zero electric field (solid line) and for  $\sim 200$  kV/cm (dotted line). The dashed line represents the difference between the transmission with and without applied electric field. The fact that the maximum transmission is limited to 30% is given by the presence of a semitransparent gold contact on the diode surface. A maximum absorption modulation of 200% is observed in the gap region.

gion gives the samples better properties homogeneity, better I-V characteristics, and makes the samples extremely stable even under high reverse bias (1 mA). The samples were all grown by molecular beam epitaxy (MBE) on (211) oriented  $\text{Cd}_{0.96}\text{Zn}_{0.04}\text{Te}$  substrates. Semitransparent gold Schottky contacts are deposited by photolithography on the sample surface.

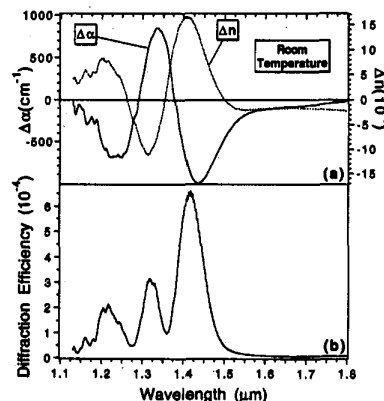
Figure 1 shows the room-temperature transmission spectra for a representative sample (with CdMgTe barriers) for different reverse electric fields. A strong absorption modulation is clearly obtained by the application of an electric field in the order of 200 kV/cm. The absorption variation reaches values as high as 200% in the region of 1.5  $\mu\text{m}$ , where the zero-field absorption is still weak.

For understanding the origin of the oscillations observed in the transmission modulation we have used a model of the electric-field effect on a bulk semiconductor (Franz-Keldysh effect).<sup>2</sup> The choice is motivated by the fact that the large wells have nearly no quantum confinement. The results we have obtained are in good agreement with the experimental ones (Fig. 2, fit to the modulation of a sample without CdMgTe barriers).

From the two transmission curves in Fig. 1 we were able to calculate the ab-



**CWF62 Fig. 2** Comparison between the experimental transmission modulation (dotted line) and the theoretical Franz-Keldysh model (solid line).



**CWF62 Fig. 3** (a)  $\Delta\alpha$  (solid line) and  $\Delta n$  (dotted line) for the sample shown in Fig. 1. (b) Calculated diffraction efficiency from the data in (a).

sorption coefficient variation  $\Delta\alpha$  as a function of the applied electric field and then, via Kramers-Kronig transformation, the corresponding variation of the refractive index,  $\Delta n$ , is obtained. The results of these calculations are shown in Fig. 3(a). The maximum  $\Delta n$  we obtain is  $\sim 1.7 \cdot 10^{-3}$ , which correspond of a relative variation in the order of  $\sim 0.05\%$ . To estimate the diffraction efficiency we used the formula reported in Ref. 3 obtaining a maximum in the gap region of  $\sim 6.5 \cdot 10^{-4}$ . The results of the calculations are shown in Fig. 3(b).

These results demonstrate that CMT-based heterostructures are good candidates for spatial light modulators in the mid-infrared.

- J. Y. Moisan, *et al.*, *Mat. Sci. Eng. B16*, 257 (1993).
- D. E. Aspnes, *Phys. Rev.* **153**, 153 (1967).
- L. Solymar, *et al.*, *Volume Holography and Volume Gratings*, (Academic Press, 1981).

### CWF63

#### Microcavity optical thyristor with strained-layer InGaAs quantum wells

G. Bickel, H. De Neve, P. Heremans, M. Kuijk,\* R. Vounckx,\* R. Baets,\*\* G. Borghs, *IMEC, Kapeldreef 75, B3001 Leuven, Belgium*

In short-distance optical interconnects such as chip-to-chip interconnects, power, area, and speed of the interconnect are critical parameters. The differential pair of optical thyristors is a unique detector/emitter device for such interconnects: a detecting pair with a total area of  $60 \times 30 \mu\text{m}^2$  has already been shown to latch with a mere 7 fJ optical input at 50 MHz.<sup>1</sup> Higher frequency operation is expected to be achieved soon. As an emitter, however, the optical thyristor is not ideal. This limits the minimum pulse width, which can still supply the required switching energy, it limits the optical fan-out, and it imposes more demands on the quality and the cost of the imaging optics.

Over the past few years the power conversion efficiency of LEDs has increased spectacularly with the help of microcavity structures. This has yielded record quantum efficiencies (QE) of 16%.<sup>2</sup> Moreover the light is more directional than a Lambertian source, which yields a higher optical throughput of any imaging optics.

In this paper, we present the first results, to our knowledge, of an NpnP optical thyristor structure embedded inside a planar microcavity. This is expected to boost the efficiency of both the emission and the detection. Additionally, the structure contains three InGaAs quantum wells (QWs) in the lower junction of the thyristor. The advantage of these QWs is twofold: it supplies light, which is not reabsorbed by the GaAs, and the QWs can be placed in the antinode of the cavity standing wave pattern, which is necessary for good resonant emission and detection.

Figure 1 shows the output spectra of